

# Transcriptome and Metabolome Changes Uncover the Potential Mechanism of High-Fat Diet Induced Obesity Under Hypoxia Condition

Mingming Fan<sup>a</sup>, Qingqing Chen<sup>b</sup>, Zhiying Xu<sup>a</sup>, Yimu Fang<sup>a</sup>, Zhuangzhi Cong<sup>a</sup>

## ABSTRACT

**Aim:** We aimed to investigate the key genes and metabolites in high-fat diet (HFD)-induced obesity model in hypoxia condition to uncover the potential mechanism.

**Method:** Mice model in control, HFD, CIH, and HFDCIH were established through diet and hypoxia treatment. Then liver tissue samples were collected for transcriptome and metabolome analysis. Following, differential analyses were conducted to select the unique genes and metabolites in HFD-induced obesity in hypoxia condition. Finally, functional analysis and correlation analysis were used to investigate the pathways and potential mechanism in obesity under hypoxia.

**Results:** A total of 448 unique genes (like CD44, FCGR4, and COL6A1) and 36 unique metabolites were identified to be affected by obesity in hypoxia condition. The function of these key genes and metabolites indicated that these genes and metabolites may be related to metabolism-related function and pathways. The interaction between these genes and metabolites may be involved in Glutathione metabolism, Arachidonic acid metabolism, Histidine metabolism, Drug metabolism-cytochrome P450.

**Conclusion:** The study uncovered the key genes and metabolites in obesity under hypoxia in mice model, and indicated the potential mechanism, providing indicator for the following focus.

## INTRODUCTION

Obesity has been considered as one of the important public health problems Blüher et al. (2019). In the past 50 years, the prevalence of obesity has increased worldwide and induce the risk of various diseases like type 2 diabetes, fatty liver, hypertension, even cancer. Obesity manifested as if imbalance between food intake and basal energy consume Gérard et al. (2016). Overconsumption of fat or fructose can induce energy metabolic disruption, mitochondria dysfunction, and autophagy dysregulation, thus inducing liver damage Chen et al. (2019).

Hypoxia affects the high-fat diet (HFD) induced obesity. Some studies considered that abnormal expansion of adipose tissue would induce endogenous hypoxia, and hypoxia stimulated inflammatory molecules secretion and contributes obesity Wang et al. (2022). Moreover, hypoxia can affect liver lipid metabolism and disturbed lipid accumulation in the liver Lefere et al. (2016). However, some studies suggested that hypoxia can improve obesity, which shows as offsetting the bodyweight and insulin resistance induced by HFD Luo et al. (2022). To fully

understand the effects of obesity on liver under hypoxia conditions, it is imperative to explore the underlying mechanism.

Transcriptome and metabolome are the important method to investigate and select the key genes and metabolites in studies. In this study, we firstly established the control, HFD, chronic intermittent hypoxia (CIH), and HFDCIH in mice, and secondly transcriptome and metabolome are used to visualize the mechanism of obesity in hypoxia condition.

## MATERIALS AND METHODS

HFD (18.1% protein, 61.6% fat and 20.3% carbohydrates; D12492) was purchased from Research Diets, Inc. Normal chow diet (NCD) (54% carbohydrate, 32% protein, 14% fat; #8604) was purchased from Teklad Rodent diet, Envigo Inc.

### Animals and groups

Male 5-week-old C57BL/6J mice were sourced from the SLAC laboratory in Shanghai, China. Male mice, aged 4

<sup>a</sup>Hepatic Surgery IV, The Third Affiliated Hospital of Naval Medical University, Shanghai, China

<sup>b</sup>Department of Prosthodontics, Shanghai Stomatological Hospital & School of Stomatology, Fudan University, Shanghai, China.

**Correspondence to:** Dr. Mingming Fan, Hepatic Surgery IV, The Third Affiliated Hospital of Naval Medical University, Shanghai, China. Email: fanmingming2024@126.com.

**Key words:** obesity; hypoxia; transcriptome; metabolome

to 6 weeks and weighing 14-16g, were housed under standardized conditions maintained at a temperature range of 22 to 24°C, with a regulated 12-hour light and 12-hour dark cycle. These animals had free access to food and water throughout the experimental period.

Twelve-eight mice were selected and randomly divided into four groups (n=3): control, HFD (high-fat diet), CIH (chronic intermittent hypoxia), and HFDCIH. Mice in control were cultured under normal oxygen condition. HFD were fed with high-fat food under normal oxygen condition. CIH were fed with normal food and were under normal oxygen condition. HFDCIH were fed with high-fat food under CIH condition. Mice in CIH were treated with intermittent hypoxia in the daytime and with normal oxygen in the night. The whole treatment lasted 24 weeks.

All experimental protocols involving animals were conducted in accordance with the ethical principles outlined in the Guide for the Care and Use of Laboratory Animals. Prior to the commencement of the study, these protocols were reviewed and approved by the Bioethics Committee of the Eastern Hepatobiliary Surgery Hospital, Second Military Medical University, ensuring compliance with the highest standards of animal welfare and ethical conduct in scientific research.

### Sample collection

After intervention, all the mice were humanely sacrificed using established protocols to minimize suffering and distress, ensuring compliance with ethical guidelines for the humane treatment of laboratory animals. Liver tissues were collected and stored at -80 °C until use.

### RNA extraction and transcriptome analysis

RNA was extracted using TRIzol® Reagent Invetrogen (Takara, Japan). Transcription and library construction were conducted in Shanghai Zhongke New Life Biotechnology Co. LTD (Shanghai, China). Gene expression was calculated using FPKM by Counts software.

### Metabolome analysis

Collected samples were involved in Ultra-performance liquid chromatography-tandem time-of-flight mass spectrometry (UHPLC-Q-TOF MS). After the sample was thawed slowly at 4°C, an appropriate amount of sample was added to the precooled methanol/acetonitrile/water solution (2:2: 1, v/v), vortexed and mixed, sonicated at low temperature for 30 min, stood at -20 °C for 10 min, centrifuged at 14000 g at 4 °C for 20 min, took the supernatant and dried under vacuum, and added 100 µL aqueous acetonitrile solution for mass spectrometry analysis (acetonitrile: Water =1:1, v/v), vortexed, centrifuged at 14000 g at 4 °C for 15 min, and the supernatant was injected for analysis.

Chromatographic condition was set as follows. Chromatographic column was Gilent 1290 Infinity LC UHPLC HILIC and column temperature was 25°C. Flow rate 0.5mL /min; the sample size was 2 µL. Mobile phases A was water + 5 mM ammonium acetate + 25 mM ammonia; mobile phases B was acetonitrile. Solvent gradient was set as follows: 95 % B (0-0.5 min), 65 % B (0.5-7 min), 40% B (7-8 min), 40 % B (8-9 min), 95 % B (9-9.1 min), and 95 % B (9.1-12min).

Q-TOF mass spectrum conditions were set as follows. Electrospray ionization (ESI) conditions of AB Triple TOF 6600 were set as follows: Ion Source Gas1 (Gas1): 60, Ion Source Gas2 (Gas2): 60, Curtain gas (CUR): 30, source temperature: 600°C, Ion Spray Voltage Floating (ISVF) ± 5500 V (Positive and negative modes); TOF MS scan m/z range: 60-1000 Da, product ion scan m/z range: 25-1000 Da, TOF MS scan accumulation time 0.20 s/spectra, product ion scan accumulation time 0.05 s/spectra. Secondary mass spectra were obtained with information dependent acquisition (IDA) and in high sensitivity mode with Declustering potential (DP): ± 60 V (positive and negative modes), Collision Energy: 35 ± 15 eV, IDA Settings as follows Exclude isotopes within 4 Da, Candidate ions to monitor per cycle: 10.

### Differential expressed genes selection

DESeq package Love et al. (2014) in R 4.1.1 was used to perform the differential expression analysis. Differential expressed genes between control and HFD, CIH and HFDCIH were identified with threshold as  $P_{adj} < 0.05$  and  $|\log_2\text{foldchange}| > 1$ . Following, VennDiagram package Chen et al. (2011) in R was conducted in the above two groups to obtain the key genes that affect the liver in obese mice under hypoxia condition. For investigating the biological functions of these key genes, they were finally involved into function analysis in Metascape database Zhou et al. (2019). Furthermore, protein-protein interaction (PPI) network and MCODE analysis were conducted.

### Differential metabolites selection

The Variable Importance for the Projection (VIP) obtained from the PLS-DA model Triba et al. (2015) model is usually used to measure the intensity of influence and the explanatory ability of the expression patterns of metabolites on the classification and discrimination of samples of each group of samples, and to explore the differential lipid molecules with biological significance. The metabolites with VIP > 1 are considered to have a significant contribution in model. Metabolomics is usually considered OPLS-DA VIP > 1 and P value < 0.05 as the screening criterion for significant difference metabolites. In this study, differential metabolites in control vs. HFD and CIH vs. HFDCIH were screened, and the differential metabolites screened by positive and negative ion modes were combined. The metabolomics enrichment analysis in

significant differential metabolites were performed in mtaboanalyst database Chong et al. (2019), Chong et al. (2018).

### Correlation analysis among differential key genes and metabolites

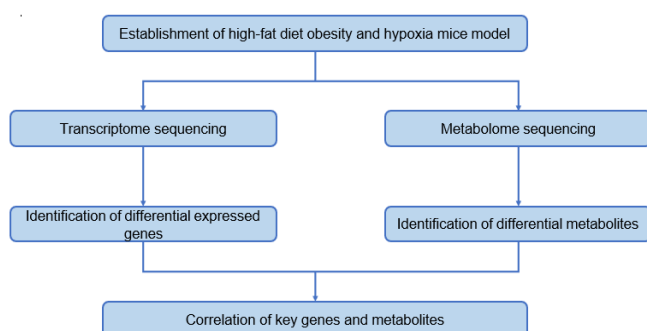
For investigating the potential mechanism of obesity under hypoxia condition, person correlation was used to explore the correlation among key genes and metabolites. Pheatmap package in R was used to visualized the results. Combined with differential gene and metabolite enrichment results, the combined pathway analysis module in mtaboanalyst database was used to conduct a comprehensive analysis of transcriptomic and metabolomic data at the level of metabolic pathways, revealing metabolic pathways and key genes affected by obesity under hypoxia conditions.

### Statistic analysis

All the above analyses were conducted in R software (version 4.1.1, R Foundation for Statistical Computing, Vienna, Austria).

The study design was showed in Figure 1.

**Figure 1:** The study designs.



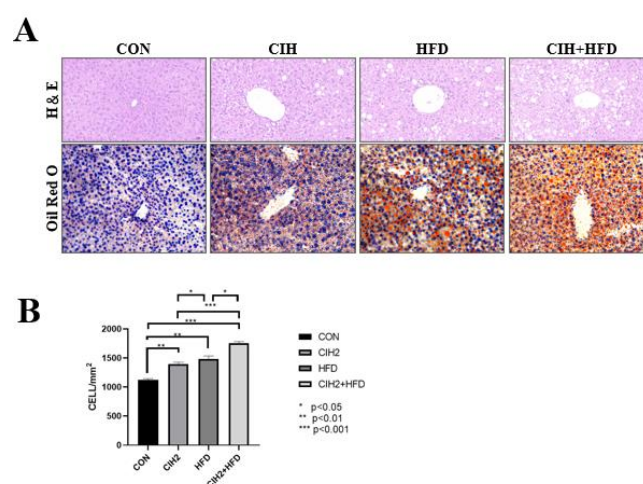
## RESULTS

### CIH promotes hepatic steatosis in normal and high-fat fed mice

We observed the morphology of healthy tissues in the Hematoxylin and Eosin staining (HE staining) and Oil Red O-staining liver slices of mice in the control group (Figure 6A). In the CIH for 2 weeks group (CIH2 group), we observed vacuolar structures surrounding the hepatic ducts in mice, uniformly distributed around the cell nuclei. Vacuolar structures were reduced in number away from the ducts. In the CIH2 group, Oil Red O staining showed more orange-red lipid droplets appearing around the hepatic ducts, notably larger in size than those in the control group. In the HFD, the presence of vacuolar structures was not correlated with the distance from the hepatic ducts, appearing uniformly in the field of view. However, the size of vacuolar structures varied, with larger

lipid droplets tending to appear further away from the ducts. Similar observations were made in Oil Red O staining, where the orange-red lipid droplets were significantly larger than those in the first two groups. In the Combined group (High-Fat Diet + Chronic Intermittent Hypoxia for 2 weeks), we found that large-sized lipid droplet vacuoles were more uniformly distributed spatially, and the number of lipid droplet vacuoles was the highest among the four groups. Oil Red O staining in the Combined group showed similar patterns to the HE-stained slices, with the observation of the largest diameter orange-red lipid droplets, and a tendency for larger lipid droplets to appear further away from the hepatic ducts Using ImageJ software for statistical analysis of the positive signal area, we found that the control group has an average area of 1120.87 mm<sup>2</sup>, the CIH2 group has an average area of 1392.15 mm<sup>2</sup>, the HFD group has an average area of 1485.54 mm<sup>2</sup>, and the CIH2+HFD group has an average area of 1755.01 mm<sup>2</sup>. Notably, compared to the control group, the experimental group shows a significant increase in stained area. Additionally, the combined group and both the CIH2 and HFD groups exhibit significant increases in area (Figure 6B).

**Figure 6:** CIH promotes hepatic lipid accumulation.



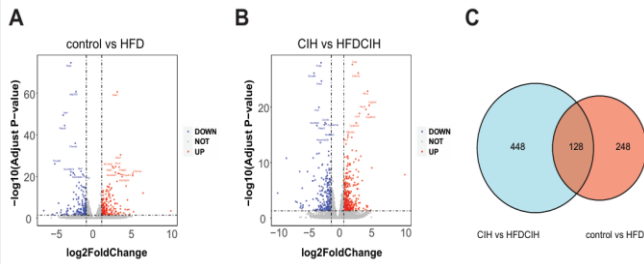
(A) A representative image of H&E(top) and Oil Red O(bottom) staining of liver sections. (B) Area of positive oil red O staining.

### Differential expressed genes

To investigate the specific mechanisms by which CIH promotes hepatic lipid accumulation in NCD- and HFD-fed mice, we performed high-throughput transcriptome sequencing of mouse liver tissue samples. A total of 376 and 576 differential expressed genes were identified in control vs. HFD and CIH vs. HFD, respectively (Figure 2A and 2B). To obtain the key genes affected by obesity under hypoxia condition, venn analysis was adopted. The 448 unique genes in CIH vs. HFD were considered as the key genes (Figure 2C).



**Figure 2:** Selection of the differential expressed genes affected by obesity in hypoxia condition.

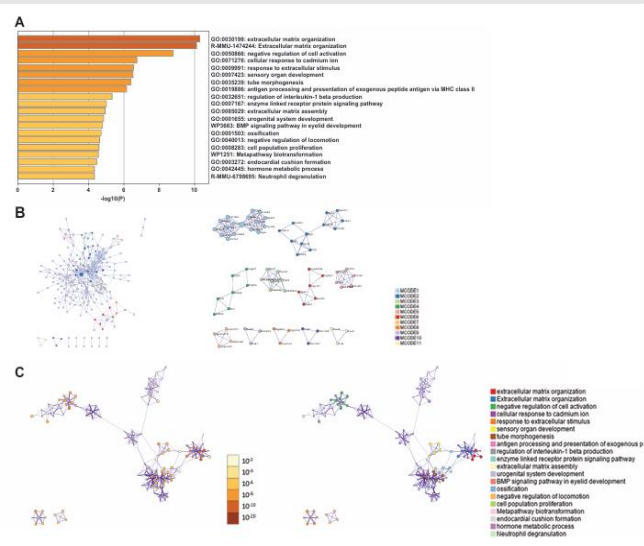


(A) Differential expressed genes between control and HFD. (B) Differential expressed genes between CIH and HFDCIH. (C) Venn analysis for selection of key genes.

Function of the key genes

For investigating the function of the above key genes affected by obesity under hypoxia condition, we performed a function enrichment analysis in these genes. The results showed that these genes were mainly related to extracellular matrix organization, negative regulation of cell activation, cellular response to cadmium ion, response to extracellular stimulus, and sensory organ development (Figure 3A) Furthermore, PPI analysis was performed to explore the interaction actions among genes (Figure 3B-C). The results suggested that these genes were closely related to each other, especially CD44, FCGR4, COL6A1, CYBB.

**Figure 3:** Function of the key genes.



(A) Function enrichment results. (B) PPI and MCODE results. (C) Pathway network. Each node presents a function pathway. Left, different colours present P value; right, different colours present different pathways.

Differential metabolites

As the threshold set in method section, 76 and 77 significantly differential metabolites were selected in

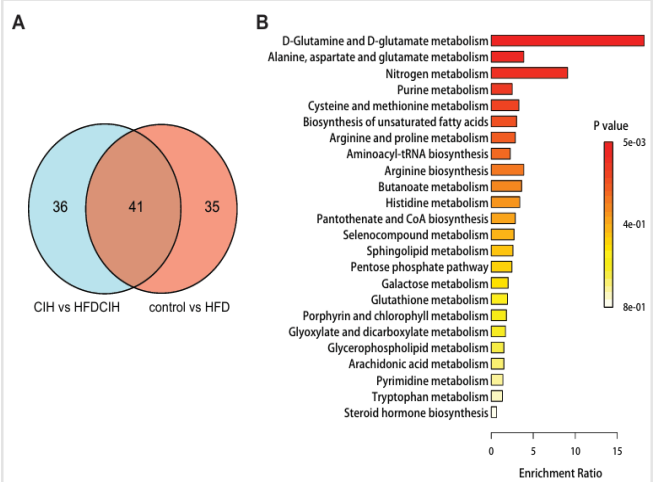
control vs. HFD and CIH vs. HFDCIH, respectively (Table 1). The 36 metabolites affected by obesity in hypoxia condition were selected through venn analysis (Figure 4A).

**Table 1:** Differential metabolites

Group	Pos/Neg	Differential metabolites	sum
Control vs HFD	Pos	48	76
	Neg	28	
CIH vs HFDCIH	Pos	51	77
	Neg	26	

**Note:** Pos, positive ion mode; Neg, negative ion mode.

**Figure 4:** Selection of the differential metabolites affected by obesity in hypoxia condition.



(A) Venn plot for selection of the metabolites. (B) Function enrichment analysis for differential metabolites.

Function of the key metabolites

For investigating the function of the key selected metabolites, we conducted a function enrichment analysis. These genes were showed tightly correlation with D-Glutamine and D-glutamate metabolism (Figure 4B).

Correlation analysis between key genes and metabolites

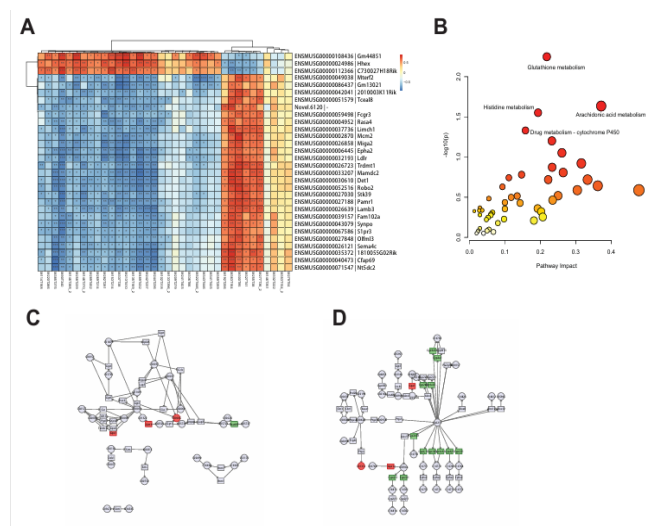
Person analysis showed that the above 448 key genes and 36 metabolites were significantly correlated. The 30 genes with the most significant correlation coefficients were screened out, and the correlation between them and 36 metabolites was visualized (Figure 5A).

The influence mechanism of obesity under hypoxia

Combined with the results of differential genes and metabolites, the transcriptome and metabolome were

used to reveal the mechanism of obesity under hypoxia conditions. Four same metabolic pathways that were significantly enriched in key genes and metabolites: Glutathione metabolism, Arachidonic acid metabolism, Histidine metabolism, Drug metabolism-cytochrome P450 (Figure 5B). The down-regulation relationship of specific genes in Glutathione metabolism and Arachidonic acid metabolism is shown in Figure 5C and D.

**Figure 5:** Correlation between the key genes and metabolites.



(A) The correlation heat plot between each key gene and metabolites. (B) Pathway enrichment analysis. X-axis, pathway impact; Y-axis, P value. (C) Glutathione metabolism pathway (left) and Arachidonic acid metabolism (right). ○, metabolite; □, gene; red, upregulation; green, downregulation.

## DISCUSSION

In this study, we established the control, HFD, CIH, and HFDCIH mice model and investigated the differential expressed genes and metabolites in control vs. HFD, and CIH vs. HFDCIH. Through intersecting the genes and metabolites in control vs. HFD, and CIH vs. HFDCIH, the unique genes and metabolites affected by obesity in hypoxia condition were finally selected. The function of these key genes and metabolites were also investigated. Based on these key genes and metabolites, we finally explored the potential mechanism of obesity in hypoxia condition.

In HFD-induced obesity mice, numerous genes act important roles. For examples, in C57BL/6 mice, HFD downregulated the UCP1, ADR3, CPT1A, ATGL, PPAR $\alpha$  expression, which are related to lipolysis and thermogenesis Luo et al. (2022). In the early process of HFD and obesity, oxygen consumption increased and adipocyte is hypoxia Lee et al. (2014). In these situation, HIF-1 $\alpha$  is active and induces tissue inflammatory and

obesity. In the present study, 448 unique genes affected by obesity in hypoxia condition were identified and these genes were mainly related to extracellular matrix organization, negative regulation of cell activation, cellular response to cadmium ion, response to extracellular stimulus, and sensory organ development. PPI analysis also showed that these genes were tightly correlated with each other.

Among these important genes, CD44, FCGR4, and COL6A1 might be the most important genes in obesity. CD44 is a cell- surface glycoprotein, is usually correlated with cell proliferation, adhesion, migration, and angiogenesis in tumor.

The recent evidences show that CD44 is also related to metabolism, especially in obesity and diabetes Weng et al. (2022). CD44, as the main receptor of the extracellular matrix component hyaluronan, has been demonstrated to mediate diet-induced insulin resistance in muscle and other insulin-sensitive tissues.

In CD44-deficient C57BL/6J mice, HFD reduced the fat mass accumulation and inflammatory biomarker expression like TNF- $\alpha$  and CD14 VerHague et al. (2022). These evidences demonstrated the regulate role of CD44 in obesity. FCGR4 is related to diagnosis of leishmaniasis Ulsan et al. (2020), whether important in obesity is absent. Collagen VI genes (COL6A1, COL6A2, and COL6A3) mutation is related to multiple muscle disease occurrence.

They also play important role in cancer, obesity, and diabetes Lamandé et al. (2018). In this study, we also found the abnormal expression of COL6A1.

Obesity is a disease closely correlated with metabolism. We further investigated the metabolome difference and finally 36 important metabolites were selected. Functional analysis showed that these metabolites were highly related to D-Glutamine and D-glutamate metabolism.

Glutamine is the most abundant free amino acid in the human body and glutamine metabolism is an important metabolic process for rapidly growing cells. In obesity, fecal glutamate and glutamate/glutamine ratio were lower than non-obesity Palomo-Buitrago et al. (2019).

For investigating the potential mechanism of HFD-induced obesity in hypoxia condition, we performed a joint analysis in the selected genes and metabolites. The present results indicated that the genes and metabolites exhibited significant correlation.

The most involved pathways contained Glutathione metabolism, Arachidonic acid metabolism, Histidine metabolism, Drug metabolism-cytochrome P450.

Overall, although we uncovered the probably mechanism of HFD-induced obesity in hypoxia, there are limitations. Firstly, the differential expressed genes and metabolites had no further optimization screening, and further studies needed to be done in this aspect. Second, the specific role of some genes needed to be explored in the further experiment like FCGR4. Thirdly, we investigated the correlation between genes and metabolites, whereas, the specific role of these genes and metabolites, as well as the correlation of them needed to be confirm in more experiments.

## CONCLUSION

Transcriptome and metabolome analysis were used to investigate the differential expressed genes and metabolites in control vs. HFD, and CIH vs. HFDCIH. The unique genes (like CD44, FCGR4, and COL6A1) and metabolites affected by obesity in hypoxia condition were finally selected. The function of these key genes and metabolites indicate that these genes and metabolites may be related to metabolism-related function and pathways. The interaction between these genes and metabolites may be involved in Glutathione metabolism, Arachidonic acid metabolism, Histidine metabolism, Drug metabolism-cytochrome P450.

## HIGHLIGHTS

1. Four hundred and forty-eight unique genes were affected by obesity under hypoxia.
2. Thirty-six unique metabolites were affected by obesity under hypoxia.
3. Obesity was related to metabolites pathways.
4. The key genes and metabolites were involved in several metabolism pathways.

## REFERENCES

1. Blüher M. 2019. Obesity: global epidemiology and pathogenesis. *Nat Rev Endocrinol.* 15(5):288-98.
2. Gérard P. 2016. Gut microbiota and obesity. *Cell Mol Life Sci.* 73(1):147-62.
3. Chen L, Lang AL, Poff GD, et al. 2019. Vinyl chloride-induced interaction of nonalcoholic and toxicant-associated steatohepatitis: Protection by the ALDH2 activator Alda-1. *Redox Biol.* 24:101205.
4. Wang R, Sun Q, Wu X, et al. 2022. Hypoxia as a Double-Edged Sword to Combat Obesity and Comorbidities. *Cells.* 11(23):3735.
5. Lefere S, Van Steenkiste C, Verhelst X, et al. 2016. Hypoxia-regulated mechanisms in the pathogenesis of obesity and non-alcoholic fatty liver disease. *Cell Mol Life Sci.* 73(18):3419-31.
6. Luo Y, Chen Q, Zou J, et al. 2022. Chronic Intermittent Hypoxia Exposure Alternative to Exercise Alleviates High-Fat-Diet-Induced Obesity and Fatty Liver. *Int J Mol Sci.* 23(9):5209.
7. Love M.I, Huber W, Anders S. 2014. Moderated estimation of fold change and dispersion for RNA-seq data with DESeq2. *Genome Biol.* 15(12):550.
8. Chen H, Boutros P.C. 2011. Venn Diagram: a package for the generation of highly-customizable Venn and Euler diagrams in R. *BMC Bioinformatics.* 12:35.
9. Zhou Y, Zhou B, Pache L, et al. 2019. Metascape provides a biologist-oriented resource for the analysis of systems-level datasets. *Nat Commun.* 10(1):1523.
10. Triba MN, Le Moyec L, Amathieu R, et al. 2015. PLS/OPLS models in metabolomics: the impact of permutation of dataset rows on the K-fold cross-validation quality parameters. *Mol Biosyst.* 11(1):13-9.
11. Chong J, Wishart DS, Xia J. 2019. Using MetaboAnalyst 4.0 for Comprehensive and Integrative Metabolomics Data Analysis. *Curr Protoc Bioinformatics.* 68(1): e86.
12. Chong J, Soufan O, Li C, et al. 2018. MetaboAnalyst 4.0: towards more transparent and integrative metabolomics analysis. *Nucleic Acids Res.* 46(W1): W486-W94.
13. Lee YS, Kim JW, Osborne O, et al. 2014. Increased adipocyte O<sub>2</sub> consumption triggers HIF-1 $\alpha$ , causing inflammation and insulin resistance in obesity. *Cell.* 157(6):1339-52.
14. Weng X, Maxwell-Warburton S, Hasib A, et al. 2022. The membrane receptor CD44: novel insights into metabolism. *Trends Endocrinol Metab.* 33(5):318-32.
15. VerHague M, Albright J, Barron K, et al. 2022. Obesogenic and diabetic effects of CD44 in mice are sexually dimorphic and dependent on genetic background. *Biol Sex Differ.* 13(1):14.
16. Ulsan Ö, Mert U, Sadiqova A, et al. 2020. Identification of gene expression profiles in Leishmania major infection by integrated bioinformatics analyses. *Acta Trop.* 208:105517.
17. Lamandé S.R, Bateman J.F. 2018. Collagen VI disorders: Insights on form and function in the extracellular matrix and beyond. *Matrix Biol.* 71-72:348-67.
18. Palomo-Buitrago ME, Sabater-Masdeu M, Moreno-Navarrete JM, et al. 2019. Glutamate interactions with obesity, insulin resistance, cognition and gut microbiota composition. *Acta Diabetol.* 56(5):569-79.